

\mathcal{PT} -symmetry breaking in a necklace of coupled optical waveguides

I V Barashenkov^{1,2}, L Baker¹, and N V Alexeeva^{1,2}

¹ *Department of Mathematics and Centre for Theoretical and Mathematical Physics, University of Cape Town, Rondebosch 7701, South Africa*

² *New Zealand Institute for Advanced Study, Massey University, Auckland 0745, New Zealand*

We consider parity-time (\mathcal{PT}) symmetric arrays formed by N optical waveguides with gain and N waveguides with loss. When the gain-loss coefficient exceeds a critical value γ_c , the \mathcal{PT} -symmetry becomes spontaneously broken. We calculate $\gamma_c(N)$ and prove that $\gamma_c \rightarrow 0$ as $N \rightarrow \infty$. In the symmetric phase, the periodic array is shown to support $2N$ solitons with different frequencies and polarisations.

PACS numbers: 42.82.Et, 11.30.Er, 11.30.Qc, 42.65.Tg, 05.45.Yv

I. INTRODUCTION

Since the emergence of the \mathcal{PT} symmetry as a research avenue in quantum theory [1], the concept was embraced in several other fields, including photonics [2], plasmonics [3], Bose-Einstein condensates [4, 5], and quantum optics of atomic gases [6]. The \mathcal{PT} -symmetric systems exhibit unusual phenomenology with a potential for practical utilisation. The \mathcal{PT} optical structures, in particular, display unconventional beam refraction [7, 8], Bragg scattering [9], nonreciprocal Bloch oscillations [10], loss-induced transparency [11], and conical diffraction [12]. Nonlinear effects in such systems can be utilised for an efficient control of light, including all-optical low-threshold switching [13, 14] and unidirectional invisibility [13, 15].

Experimentally, the optical \mathcal{PT} symmetry was realised in a directional coupler consisting of two coupled waveguides with gain and loss [2, 11], and in chains of such dipoles [16]. The corresponding theoretical models went on to include the effects of diffraction of spatial beams and dispersion of temporal pulses, i.e., include an additional spatial or temporal dimension [17]. Dispersive \mathcal{PT} -couplers were shown to support optical solitons [17, 18]. Triplets, quadruplets and quintets of (nondispersive) guides were also dealt with [19].

A fundamental phenomenon observed in symmetric couplers is the spontaneous \mathcal{PT} -symmetry breaking [2, 15–17, 20] which occurs as the gain-loss coefficient is increased beyond a certain critical value γ_c . This exceptional point separates the symmetric phase, where all perturbation frequencies are real, and the symmetry-broken phase, where some frequencies are complex and the corresponding modes grow exponentially. Besides demarcating the stability boundary, the exceptional point has several other roles to play. In particular, it is in the vicinity of this critical value that the \mathcal{PT} -symmetric periodic structures can act as unidirectional invisible media [15].

In this paper, we consider a generalisation of the two-channel dispersive coupler to a \mathcal{PT} -symmetric arrangement of $2N$ dispersive waveguides coupled to their nearest neighbours — see fig.1. (The previously analysed situation corresponds to $N = 1$ [17, 18].) The issue that

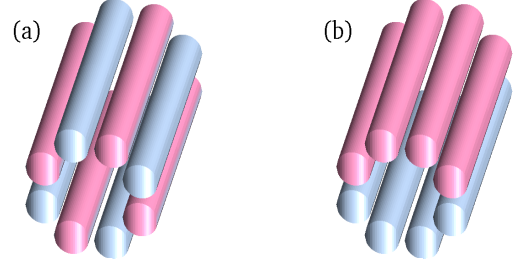


FIG. 1. (Color) An alternating (a) and clustered (b) necklace of waveguides with gain (pink) and loss (blue).

concerns us here, is how the geometry of this system and the growing multiplicity of its channels affects the symmetry-breaking point, γ_c . We also uncover the diversity of solitons arising in such a chain.

The chain consists of N waveguides with gain and N with loss. The complex mode amplitudes, u_n , satisfy

$$i\dot{u}_n + u_n'' + 2|u_n|^2 u_n + u_{n-1} + u_{n+1} = 2i\Gamma_n u_n \quad (n = 1, \dots, 2N), \quad (1)$$

where $\dot{u}_n \equiv \partial u_n / \partial t$ and $u_n'' \equiv \partial^2 u_n / \partial z^2$. In Eq.(1), t stands for time and z for the distance in the frame of reference traveling along with the pulse. The coefficient Γ_n equals $\gamma > 0$ for the waveguides with gain and $-\gamma$ for those with loss. The active and lossy guides are either separated into two clusters or simply alternate (fig.1). The chain forms a periodic necklace, that is, $u_{2N+1} = u_1$ and $u_0 = u_{2N}$.

We also consider open chains. An open chain is described by Eqs.(1) without the periodicity condition:

$$\begin{aligned} i\dot{u}_1 + u_1'' + 2|u_1|^2 u_1 + u_2 &= 2i\gamma u_1, \\ i\dot{u}_{2N} + u_{2N}'' + 2|u_{2N}|^2 u_{2N} + u_{2N-1} &= -2i\gamma u_{2N}, \\ i\dot{u}_n + u_n'' + 2|u_n|^2 u_n + u_{n-1} + u_{n+1} &= 2i\Gamma_n u_n \\ &\quad (n = 2, \dots, 2N - 1). \end{aligned} \quad (2)$$

With a suitably chosen constant matrix \mathcal{L} , Eqs.(1)-(2)

can be written in a unified way:

$$i\dot{u}_n + u_n'' + \sum_{m=1}^{2N} \mathcal{L}_{nm} u_m + 2|u_n|^2 u_n = 0. \quad (3)$$

Of particular importance for dispersive waveguides is the zero solution of Eq.(3), $u_n(z, t) = 0$ ($n = 1, \dots, 2N$). This solution shall serve as a background to solitons [17] and breathers [18]. To classify its stability, we linearise (3) and let $u_n = c_n e^{i(kz - \omega t)}$, where k and ω are assumed to be real. The combination $\lambda = k^2 - \omega$ is then found as an eigenvalue of the linearisation matrix \mathcal{L} . The zero solution loses stability when two real eigenvalues merge and become a complex-conjugate pair.

It is fitting to note that an equivalent eigenvalue problem arises in the linearisation of the trivial solution of the symmetric array of *nondispersive* (z -independent) waveguides. [The nondispersive array is a lattice system defined by Eq.(3) without the u_n'' term.] The $N = 1$ case corresponds to the \mathcal{PT} -symmetric nondispersive coupler (also referred to as the dimer) [4, 13, 14]. The $N = 2$ case (the \mathcal{PT} -quadrimer) was considered in [19].

II. OPEN ALTERNATING CHAIN

The alternating necklaces have $\Gamma_n = (-1)^{n+1} \gamma$ for $n = 1, \dots, 2N$. It is convenient to consider the *open* chain first. In this case,

$$\mathcal{L}_{nm} = -2i\Gamma_n \delta_{n-m} + \delta_{n-m-1} + \delta_{n-m+1}, \quad (4)$$

$n, m = 1, \dots, 2N$. Here δ is the Kronecker delta symbol:

$$\delta_n = \begin{cases} 1, & \text{if } n = 0; \\ 0 & \text{otherwise.} \end{cases}$$

The stability eigenvalues are expressible via roots of the secular equation $\mathcal{D}_{2N}(\gamma, \alpha) = 0$, where $\lambda = -2\alpha$ and

$$\mathcal{D}_{2N} = \det(\mathcal{L} + 2\alpha I). \quad (5)$$

The determinants with $N = 1$ and 2 are readily found:

$$\begin{aligned} \mathcal{D}_2 &= 2x + 1; \\ \mathcal{D}_4 &= 4x^2 + 2x - 1, \end{aligned}$$

where $x = 2(\gamma^2 + \alpha^2) - 1$. Any determinant with $N \geq 3$ can be expanded as

$$\mathcal{D}_{2N} = 2x\mathcal{D}_{2(N-1)} - \mathcal{D}_{2(N-2)}. \quad (6)$$

The recursion relation (6) with $\mathcal{D}_2 = 2x + 1$ and $\mathcal{D}_4 = 4x^2 + 2x - 1$ admits a simple solution

$$\mathcal{D}_{2N}(\gamma, \alpha) = U_N(x) + U_{N-1}(x), \quad (7)$$

where $U_N(x)$ is the Chebyshev polynomial of the second kind of N th order [21]. Using the defining property of the Chebyshev polynomials,

$$U_N(x) = \frac{\sin[(N+1)\theta]}{\sin\theta}, \quad \text{where } x = \cos\theta,$$

we evaluate the determinant \mathcal{D}_{2N} as

$$\mathcal{D}_{2N} = \frac{\sin[(2N+1)\theta/2]}{\sin(\theta/2)}. \quad (8)$$

\mathcal{D}_{2N} has $2N$ simple roots

$$\theta_n = \pm \frac{2n}{2N+1} \pi, \quad n = 1, 2, \dots, N.$$

On the (γ, α) -plane, equations $\gamma^2 + \alpha^2 = \cos^2(\theta_n/2)$ describe N concentric circles centred at the origin. As γ grows through $\gamma_n = \cos(\theta_n/2)$, two opposite eigenvalues $\lambda = -2\alpha$ converge at $\lambda = 0$ and become complex. The \mathcal{PT} -symmetry breaking threshold is determined by the γ -intercept of the smallest circle: $\gamma_c = \cos(\theta_N/2)$, i.e.,

$$\gamma_c = \sin \frac{\pi}{2(2N+1)}. \quad (9)$$

III. PERIODIC ALTERNATING CHAIN

Linearising the periodic alternating necklace (1), the corresponding secular equation is $\tilde{\mathcal{D}}_{2N}(\gamma, \alpha) = 0$, where

$$\tilde{\mathcal{D}}_{2N} = \det(\tilde{\mathcal{L}} + 2\alpha I).$$

The matrix $\tilde{\mathcal{L}}$ is given by the same expression (4), with the same $\Gamma_n = (-1)^{n+1} \gamma$, but with δ replaced with the *cyclic* Kronecker symbol $\delta^{(2N)}$:

$$\delta_n^{(2N)} = \begin{cases} 1, & \text{if } n \bmod 2N = 0; \\ 0 & \text{otherwise.} \end{cases}$$

The determinant $\tilde{\mathcal{D}}_{2N}$ can be expressed via the “nonperiodic” determinants (5):

$$\tilde{\mathcal{D}}_{2N} = \mathcal{D}_{2N} - \mathcal{D}_{2(N-1)} - 2.$$

Using (8) the determinant in question is evaluated to be

$$\tilde{\mathcal{D}}_{2N} = -4 \sin^2(N\theta/2),$$

with the double roots $\theta_n = \frac{2n}{N} \pi$, $n = 1, 2, \dots, N$.

As in the open-necklace case, equations

$$\gamma^2 + \alpha^2 = \cos^2(\theta_n/2)$$

describe concentric circles on the (γ, α) -plane. When N is even, the smallest circle corresponds to $n = N/2$ and has zero radius. When N is odd, the smallest circle corresponds to $n = \frac{1}{2}(N-1)$; the radius in this case is $\sin[\pi/(2N)]$. Thus,

$$\gamma_c = \begin{cases} 0, & N = \text{even}; \\ \sin\left(\frac{\pi}{2N}\right), & N = \text{odd}. \end{cases} \quad (10)$$

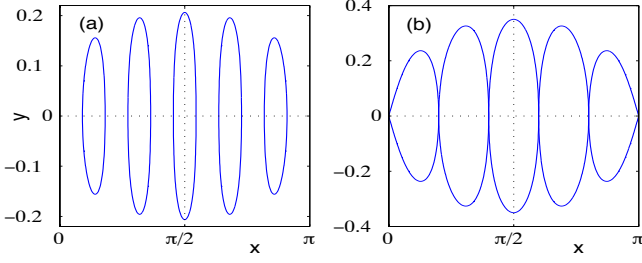


FIG. 2. (Color online) The implicit curves (12) (a) and (19) (b), in the interval $0 \leq x \leq \pi$. In both panels, $N = 5$.

IV. OPEN CLUSTERED NECKLACE

When the waveguides are grouped into two clusters, the gain-loss coefficient Γ_n equals $\gamma > 0$ for $n = 1, \dots, N$ and $-\gamma$ for $n = N + 1, \dots, 2N$. Again, we start with the open chain, Eq.(2). The corresponding linearisation matrix \mathcal{L} is as in Eq.(4).

To find roots of the corresponding secular equation $\Delta_{2N} = 0$, where $\Delta_{2N} = \det(\mathcal{L} + 2\alpha I)$, we expand

$$\Delta_{2N}(\gamma, \alpha) = U_N(\zeta)U_N^*(\zeta) - U_{N-1}(\zeta)U_{N-1}^*(\zeta), \quad (11)$$

where U_N is a determinant of an $N \times N$ tridiagonal matrix

$$U_{m,n} = 2\zeta\delta_{m-n} + \delta_{|m-n|-1} \quad (m, n = 1, 2, \dots, N),$$

and $\zeta = \alpha - i\gamma$. This determinant is nothing but the Chebyshev polynomial (of the complex argument); hence our choice of notation [21]. Defining complex θ , such that $\zeta = \cos \theta$, the Chebyshev polynomial can be written as

$$U_N(\zeta) = \frac{\sin[(N+1)\theta]}{\sin \theta}.$$

Letting $\theta = x + iy$, the secular equation reduces to

$$\sinh y \sinh[(2N+1)y] = -\sin x \sin[(2N+1)x]. \quad (12)$$

Here $x^2 + y^2 \neq 0$ (for $\theta = 0$ is not a root of $\Delta_{2N} = 0$). Note that x and y are the elliptic coordinates on the (γ, α) plane:

$$\alpha = \cos x \cosh y, \quad \gamma = \sin x \sinh y. \quad (13)$$

The right-hand side of (12) is π -periodic; hence it is sufficient to consider the interval $0 \leq x \leq \pi$. The curve described by (12) consists of N disconnected ovals in subintervals

$$\frac{2n-1}{2N+1}\pi \leq x \leq \frac{2n}{2N+1}\pi, \quad n = 1, \dots, N$$

[fig.2(a)]. The transformation (13) maps these to N ovals on the (γ, α) -plane [shown in fig.3(a)]. Of interest to us are the points where pairs of $\alpha(\gamma)$ branches merge.

In Eq.(12), the sinusoid $\sin(2N+1)x$ is modulated by a slowly changing amplitude $\sin x$. Therefore, of all

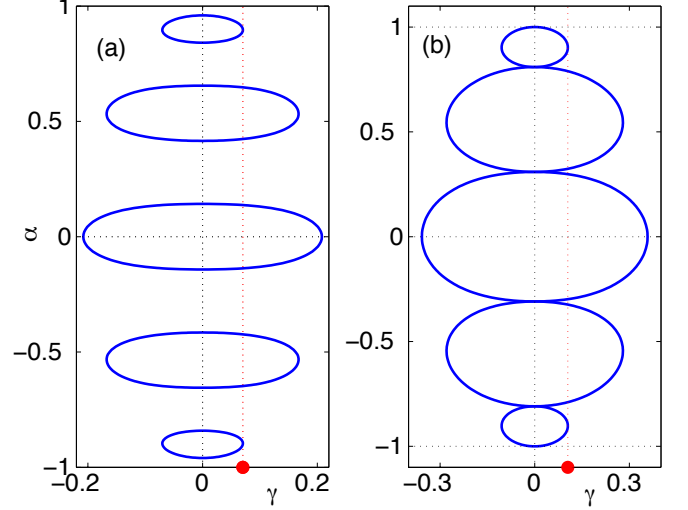


FIG. 3. (Color online) The curve $\Delta_{2N}(\alpha, \gamma) = 0$ (a) and $\tilde{\Delta}_{2N}(\alpha, \gamma) = 0$ (b) with Δ_{2N} and $\tilde{\Delta}_{2N}$ as in (11) and (18). (Here $N = 5$.) The red dot on the γ -axis marks γ_c , the point of the \mathcal{PT} -symmetry breaking.

N ovals, the first and the last one (those with $n = 1$ and $n = N$) have the lowest maximum values of y . The transformation $(x, y) \rightarrow (x, \gamma)$, where $\gamma = \sin x \sinh y$, keeps the pattern horizontally periodic but elongates the central ovals still further. Therefore, the lowest value of γ for which the merger of two real eigenvalues $\lambda = -2\alpha(\gamma)$ occurs, corresponds to the apogee of the first and the last $\gamma(x)$ ovals. Using (12), the condition $d\gamma/dx = 0$ translates into

$$\frac{\tanh y}{\tan x} = \frac{[\sin x \sin(2N+1)x]_x}{[\sinh y \sinh(2N+1)y]_y}. \quad (14)$$

One can readily construct asymptotic roots of the system (12), (14), as $N \rightarrow \infty$. Expanding x and y in powers of $\frac{1}{2N+1}$, Eqs.(12) and (14) give, respectively:

$$\xi \sinh \xi = -\mathcal{S} \eta \sin \eta, \quad (15)$$

$$\xi(\sinh \xi + \xi \cosh \xi) = \mathcal{S} \eta(\sin \eta + \eta \cos \eta), \quad (16)$$

where

$$x = \frac{\eta}{2N+1} + \dots, \quad y = \frac{\xi}{2N+1} + \dots,$$

and $\mathcal{S} = 1$.

The system (15)-(16) has an increasing sequence of roots $\eta_n, \xi_n > 0$, $n = 1, 2, \dots$ [See fig.4(a).] In particular, $\eta_1 = 5.33$, $\xi_1 = 1.68$. Hence we get, for each N ,

$$x_n^{(N)} = \frac{\eta_n}{2N+1} + \dots, \quad y_n^{(N)} = \frac{\xi_n}{2N+1} + \dots,$$

where “...” stand for corrections of order $(2N+1)^{-2}$. (These asymptotic expressions are accurate for n such that η_n and ξ_n are much smaller than $2N+1$.)

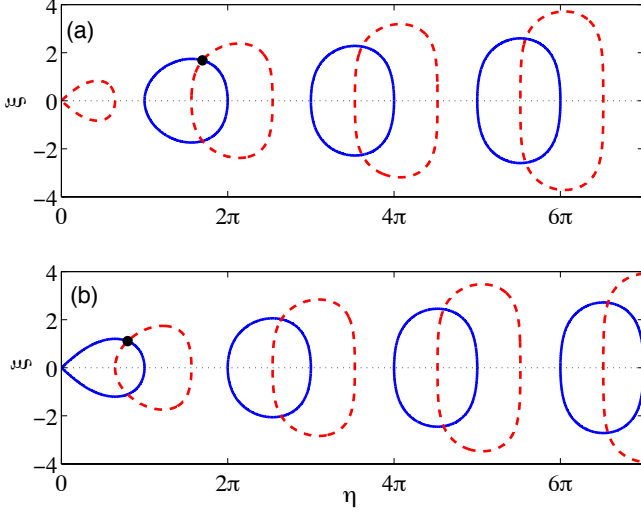


FIG. 4. (Color online) The graphical solution of the system (15)-(16) with $\mathcal{S} = 1$ (a) and $\mathcal{S} = -1$ (b). The blue (solid) and red (broken) curve are described by equation (15) and (16), respectively. The black dot marks the root (η_1, ξ_1) in (a), and the root $(\tilde{\eta}_1, \tilde{\xi}_1)$ in (b).

The corresponding values γ_n are recovered from (13). Of primary importance is the smallest value γ_1 which determines the symmetry breaking threshold: $\gamma_c = \gamma_1 = \eta_1 \xi_1 (2N+1)^{-2} + \dots$. Substituting for η_1 and ξ_1 , we get

$$\gamma_c = \frac{8.95}{(2N+1)^2} + O\left(\frac{1}{(2N+1)^3}\right) \quad \text{as } N \rightarrow \infty. \quad (17)$$

V. PERIODIC CLUSTERED NECKLACE

The closed clustered chain is described by Eq.(1) with $\Gamma_n = \gamma > 0$ ($n = 1, 2, \dots, N$) and $\Gamma_n = -\gamma$ ($n = N+1, \dots, 2N$). The \mathcal{L} -matrix is

$$\mathcal{L}_{nm} = -2i\Gamma_n \delta_{n-m}^{(2N)} + \delta_{n-m-1}^{(2N)} + \delta_{n-m+1}^{(2N)},$$

$n, m = 1, \dots, 2N$.

The characteristic determinant is expandable as

$$\tilde{\Delta}_{2N} = U_N U_N^* - 2U_{N-1} U_{N-1}^* + U_{N-2} U_{N-2}^* - 2, \quad (18)$$

where $U_N(\zeta)$ is the Chebyshev polynomial of $\zeta = \alpha - i\gamma$. Using the elliptic coordinates (13), $\tilde{\Delta}_{2N} = 0$ reduces to

$$\sinh(Ny) \sinh y = |\sin(Nx) \sin x|. \quad (19)$$

Because of the periodicity of the right-hand side of (19), it is sufficient to consider the interval $0 \leq x < \pi$. The curve (19) consists of N ovals [fig.2(b)]: one in each of the subintervals

$$\frac{2(n-1)}{N}\pi \leq x \leq \frac{2n-1}{N}\pi, \quad n = 1, \dots, \left[\frac{N+1}{2}\right]$$

and one in each of the complementary subintervals

$$\frac{2n-1}{N}\pi \leq x \leq \frac{2n}{N}\pi, \quad n = 1, \dots, \left[\frac{N}{2}\right].$$

(Here $[p]$ indicates the integer part of p .) The former set will be referred to as *even* ovals, and the latter one as *odd*.

When N is large, one can find the maximum value of the function $\gamma(x)$ in each subinterval as an expansion in powers of $\frac{1}{N}$. The lowest maximum γ_1 in the *odd* set is given by $\eta_1 \xi_1 N^{-2} + O(N^{-3})$, where η_1, ξ_1 is the first pair of roots of the system (15)-(16) with $\mathcal{S} = 1$. Substituting their numerical values, we obtain $\gamma_1 = 8.95N^{-2} + \dots$

The lowest maximum in the *even* set is given by $\tilde{\gamma}_1 = \tilde{\eta}_1 \tilde{\xi}_1 N^{-2} + \dots$, where $\tilde{\eta}_1 = 2.50, \tilde{\xi}_1 = 1.11$ is the first pair of roots of the system (15)-(16) with $\mathcal{S} = -1$. The maximum $\tilde{\gamma}_1$ is lower than γ_1 ; hence it is $\tilde{\gamma}_1$ that determines the symmetry-breaking threshold of the closed clustered necklace. Substituting for $\tilde{\eta}_1, \tilde{\xi}_1$, we finally get

$$\gamma_c = 2.77 N^{-2} + O(N^{-3}) \quad \text{as } N \rightarrow \infty. \quad (20)$$

VI. SOLITONS

Assume the \mathcal{PT} symmetry is unbroken, $\gamma < \gamma_c$. Let $\vec{\phi}_n$ be an eigenvector of \mathcal{L} pertaining to the (real) eigenvalue λ_n . The transformation $u_n = \sum \Phi_{nm} \psi_m$, with $\Phi = \{\vec{\phi}_1, \vec{\phi}_2, \dots, \vec{\phi}_{2N}\}$, casts Eq.(3) in the form

$$i\psi_\ell + \psi_\ell'' + \lambda_\ell \psi_\ell + 2 \sum_{n,m} (\Phi^{-1})_{\ell n} \mathcal{N}_n \Phi_{nm} \psi_m = 0, \quad (21)$$

where

$$\mathcal{N}_n = |\sum \Phi_{nm} \psi_m|^2.$$

(Physically, $\mathcal{N}_n = |u_n|^2$ has the meaning of the power density in the n -th waveguide.) We will show that the vector equation (21) admits $2N$ independent scalar reductions.

In this paper, we confine our consideration to the case of the periodic alternating chain, Eq.(1) with $\Gamma_n = (-1)^{n+1}\gamma$. The corresponding matrix \mathcal{L} has 2 simple and $N-1$ double eigenvalues. The simple eigenvalues $\lambda_\pm = \pm 2 \cos \vartheta$ have eigenvectors

$$\vec{\phi}_\pm = (1, \pm e^{\pm i\vartheta}, 1, \pm e^{\pm i\vartheta}, \dots),$$

where $\sin \vartheta = \gamma$. These satisfy $|(\vec{\phi}_\pm)_j| = 1$, for all j . We now show that the rest of the eigenvectors can also be chosen to satisfy this property.

The matrix \mathcal{L} commutes with the \mathbb{Z}_N -rotation \mathcal{R} , where $\mathcal{R}_{nm} = \delta_{n-m-2}^{(2N)}$. Therefore the basis in the invariant subspace S_n associated with the eigenvalue λ_n can be chosen in the form of two eigenvectors of \mathcal{R} :

$$\mathcal{R}\vec{\psi}_1 = e^{2\pi i/N} \vec{\psi}_1, \quad \mathcal{R}\vec{\psi}_2 = e^{-2\pi i/N} \vec{\psi}_2. \quad (22)$$

The linearisation matrix satisfies $\mathcal{L}\mathcal{P} = \mathcal{P}\mathcal{L}^*$, where \mathcal{P} is the inversion:

$$\mathcal{P}_{nm} = \delta_{n+m-1}^{(2N)}.$$

Therefore, $\mathcal{P}\vec{\psi}_1^*$ and $\mathcal{P}\vec{\psi}_2^*$ are also in S_n . Since $\mathcal{R}\mathcal{P} = \mathcal{P}\mathcal{R}^{-1}$, the vector $\mathcal{P}\vec{\psi}_1^*$ is an eigenvector of the rotation \mathcal{R} , with an eigenvalue $e^{2\pi i/N}$. That is, $\mathcal{P}\vec{\psi}_1^* = C\vec{\psi}_1$, with some constant C . Since $\mathcal{P}^2 = I$, the constant $C = e^{i\chi}$, with χ real. Thus,

$$\mathcal{P}\vec{\psi}_1^* = e^{i\chi}\vec{\psi}_1, \quad \mathcal{P}\vec{\psi}_2^* = e^{-i\chi}\vec{\psi}_2. \quad (23)$$

We normalise $\vec{\psi}_1, \vec{\psi}_2$ so that $(\vec{\psi}_1)_1 = (\vec{\psi}_2)_1 = 1$. Eq.(22) tells us that

$$(\vec{\psi}_1)_{1+2\ell} = e^{-2\pi i\ell/N}, \quad (\vec{\psi}_2)_{1+2\ell} = e^{2\pi i\ell/N}, \quad \ell = 1, 2, \dots$$

On the other hand, Eq.(23) gives

$$(\vec{\psi}_1)_{2N-2\ell} = e^{-i\chi+2\pi i\ell/N}, \quad (\vec{\psi}_2)_{2N-2\ell} = e^{i\chi-2\pi i\ell/N}.$$

Thus all eigenvectors of \mathcal{L} have unimodular components:

$$|\Phi_{nm}| = |(\vec{\phi}_m)_n| = 1; \quad n, m = 1, 2, \dots, 2N. \quad (24)$$

Returning to (21), the scalar reduction is defined by letting $\psi_m = \psi\delta_{m-M}$, with some fixed M . In view of (24), this gives $\mathcal{N}_n = |\psi|^2$ for all n . All components of (21) become identically zero, except the one with $\ell = M$, which becomes

$$i\dot{\psi} + \psi'' + \lambda_M\psi + 2|\psi|^2\psi = 0. \quad (25)$$

Each nonlinear Schrödinger equation (25), with $M = 1, \dots, 2N$, supports a soliton

$$\psi = e^{i\Omega t} a \operatorname{sech}(az),$$

with the frequency $\Omega = a^2 + \lambda_M$. Thus the original \mathcal{PT} -symmetric system (1) has $2N$ coexisting soliton solutions, different in their frequencies and polarisations.

We should emphase the difference between these vector solitons and (spatial) solitons in a \mathcal{PT} -symmetric optical

lattice [22]. While the solitons in the waveguide necklace (1) are localised as functions of z , the lattice solitons [22] are localised as functions of n (i.e., in the transverse direction). The n dependence determines the power density distribution over the $2N$ channels; this distribution is uniform in the case of the vector solitons of Eq.(1).

VII. CONCLUDING REMARKS

In conclusion, we have determined the symmetry breaking points for four different geometries of the necklace. Generically, there is a finite interval of the gain-loss coefficient where the \mathcal{PT} symmetry is unbroken. The only exception is the periodic chain of $2N$ alternating waveguides with even N . Here $\gamma_c = 0$, i.e., the symmetry is spontaneously broken for an arbitrarily small γ .

The *alternating* arrays admit an explicit solution; the transition points are given by (9) for the open chains and by (10) for the periodic necklaces. In both cases $\gamma_c \sim \frac{1}{N}$ for large N . In the *clustered* geometry, the threshold values are expressible via roots of a simple transcendental equation — Eq.(12) in the case of the open chain, and Eq.(19) in the periodic situation. Eqs.(17) and (20) yield the corresponding asymptotic results. Here, the \mathcal{PT} symmetry breaks quicker: $\gamma_c \sim \frac{1}{N^2}$ as $N \rightarrow \infty$.

It is interesting to note that a similar $\gamma_c \sim \frac{1}{N^2}$ law was detected in a *disordered* \mathcal{PT} -symmetric chain with the clustered arrangement of gain and loss, in the limit of large localisation lengths of the eigenmodes [23].

Our $\gamma_c(N)$ values remain valid for the arrays of *nondispersive* \mathcal{PT} -symmetric couplers [Eqs.(1)-(2) without the u_n'' term]. In particular, our conclusion that the limit of the sequence $\gamma_c(N)$ as $N \rightarrow \infty$ exists and equals 0, is in agreement with the symmetry-breaking threshold for the infinite alternating chain [24].

Finally, we have demonstrated that the alternating periodic necklace supports $2N$ coexisting soliton solutions. These vector solitons are characterised by the uniform distribution of the power density over their $2N$ components and are different in their frequencies and polarisations. It is natural to expect that the other three \mathcal{PT} -symmetric waveguide arrangements (open-alternating, open- and periodic-clustered) will also exhibit $2N$ different solitons each.

REFERENCES

-
- [1] C. M. Bender and S. Boettcher, Phys. Rev. Lett. **80**, 5243 (1998); C. M. Bender, Rep. Prog. Phys. **70**, 947 (2007)
 - [2] C.E. Rüter, K.G. Makris, R. El-Ganainy, D.N. Christodoulides, M. Segev, D. Kip, Nat. Phys. **6** 192 (2010)
 - [3] H. Benisty, A. Degiron, A. Lupu, A. De Lustrac, S. Chénais, S. Forget, M. Besbes, G. Barbillon, A. Bruyant, S. Blaize, and G. Lérondel, Opt. Express **19**, 18004 (2011)
 - [4] E.M. Graefe, H. J. Korsch, and A. E. Niederle, Phys. Rev.

- Lett. **101** 150408 (2008); E.M. Graefe, H. J. Korsch, and A. E. Niederle, Phys. Rev. A **82**, 013629 (2010)
- [5] H. Cartarius and G. Wunner, Phys. Rev. A **86** 013612 (2012); A. S. Rodrigues, K. Li, V. Achilleos, P. G. Kevrekidis, D. J. Frantzeskakis, and C. M. Bender, arXiv: 1207.1066 (2012)
- [6] C. Hang, G. Huang, and V. V. Konotop, arXiv: 1212.5486 (2012)
- [7] K.G. Makris, R. El-Ganainy, D.N. Christodoulides, Z.H. Musslimani, Phys. Rev. Lett. **100** 103904 (2008)
- [8] M.C. Zheng, D.N. Christodoulides, R. Fleischmann, T. Kottos, Phys. Rev. A **82** 010103 (2010)
- [9] M.V. Berry, J. Phys. A **41** 244007 (2008); S. Longhi, Phys. Rev. A **81** 022102 (2010)
- [10] S. Longhi, Phys. Rev. Lett. **103** 123601 (2009)
- [11] A. Guo, G. J. Salamo, D. Duchesne, R. Morandotti, M. Volatier-Ravat, V. Aimez, G. A. Siviloglou, and D. N. Christodoulides, Phys. Rev. Lett. **103** 093902 (2009)
- [12] H. Ramezani, T. Kottos, V. Kovanis, D. N. Christodoulides, Phys. Rev. A **85** 013818 (2012)
- [13] H. Ramezani, T. Kottos, R. El-Ganainy, D.H. Christodoulides, Phys. Rev. A **82** 043803 (2010)
- [14] A.A. Sukhorukov, Z.Y. Xu, Yu.S. Kivshar, Phys. Rev. A **82** 043818 (2010)
- [15] Z. Lin, H. Ramezani, T. Eichelkraut, T. Kottos, H. Cao, and D.N. Christodoulides, Phys. Rev. Lett. **106** 213901 (2011)
- [16] A. Regensburger, C. Bersch, M.-A. Miri, G. Onishchukov, D.N. Christodoulides, and U. Peschel, Nature **488** 167 (2012)
- [17] S.V. Suchkov, B.A. Malomed, S.V. Dmitriev, and Y.S. Kivshar, Phys. Rev. E **84** 046609 (2011); R. Driben and B.A. Malomed, Opt. Lett. **36** 4323 (2011); R. Driben and B.A. Malomed, EPL **96** 51001 (2011); N.V. Alexeeva, I. V. Barashenkov, A. A. Sukhorukov, and Y.S. Kivshar, Phys. Rev. A **85** 063837 (2012); Y. Li, J. Liu, W. Pang, and B.A. Malomed, Phys. Rev. A **87** 013604 (2013); Yu. V. Bludov, V. V. Konotop, and B. A. Malomed, Phys. Rev. A **87** 013816 (2013)
- [18] I.V. Barashenkov, S.V. Suchkov, A.A. Sukhorukov, S.V. Dmitriev, and Y.S. Kivshar, Phys. Rev. A **86** 053809 (2012)
- [19] K. Li and P.G. Kevrekidis, Phys. Rev. E **83** 066608 (2011); D.A. Zezyulin and V.V. Konotop, Phys. Rev. Lett. **108** 213906 (2012); K. Li, P.G. Kevrekidis, B.A. Malomed, and U. Günther, J. Phys. A: Math. Theor. **45** 444021 (2012)
- [20] S. Klaiman, U. Günther, N. Moiseyev, Phys. Rev. Lett. **101** 080402 (2008)
- [21] G. Szegő, Orthogonal Polynomials. American Mathematical Society, Providence (1975)
- [22] Z. H. Musslimani, K.G. Makris, R. El-Ganainy, and D.N. Christodoulides, Phys. Rev. Lett. **100** 030402 (2008); V. V. Konotop, D. E. Pelinovsky and D. A. Zezyulin, EPL **100** 56006 (2012); Y. He and D. Mihalache, J. Opt. Soc. Am. B **29** 2554 (2012); Y. He and D. Mihalache, Phys. Rev. A **87** 013812 (2013)
- [23] O. Bendix, R. Fleischmann, T. Kottos, B. Shapiro, Phys. Rev. Lett. **103** 030402 (2009)
- [24] S.V. Dmitriev, A.A. Sukhorukov, and Y.S. Kivshar, Opt. Lett. **35** 2976 (2010)